



XTX101, a tumor-activated, Fc-enhanced anti-CTLA-4 monoclonal antibody, demonstrates tumor-growth inhibition and tumor-selective pharmacodynamics in mouse models of cancer

Kurt A Jenkins ^{1,2}, Miso Park,² Magali Pederzoli-Ribeil,¹ Ugur Eskiocak,¹ Parker Johnson,^{1,2} Wilson Guzman,¹ Megan McLaughlin,¹ Deborah Moore-Lai,¹ Caitlin O'Toole,¹ Zhen Liu,¹ Benjamin Nicholson,¹ Veronica Flesch,² Huawei Qiu,¹ Tim Clackson,¹ Ronan C O'Hagan,¹ Ulrich Rodeck,³ Margaret Karow,¹ Jennifer O'Neil,¹ John C Williams ²

To cite: Jenkins KA, Park M, Pederzoli-Ribeil M, *et al.* XTX101, a tumor-activated, Fc-enhanced anti-CTLA-4 monoclonal antibody, demonstrates tumor-growth inhibition and tumor-selective pharmacodynamics in mouse models of cancer. *Journal for ImmunoTherapy of Cancer* 2023;11:e007785. doi:10.1136/jitc-2023-007785

► Additional supplemental material is published online only. To view, please visit the journal online (<http://dx.doi.org/10.1136/jitc-2023-007785>).

Accepted 09 November 2023



© Author(s) (or their employer(s)) 2023. Re-use permitted under CC BY-NC. No commercial re-use. See rights and permissions. Published by BMJ.

¹Xilio Therapeutics, Waltham, Massachusetts, USA

²Molecular Medicine, City of Hope National Medical Center, Beckman Research Institute, Duarte, California, USA

³Department of Dermatology and Cutaneous Biology, Thomas Jefferson University, Philadelphia, Pennsylvania, USA

Correspondence to

Dr Kurt A Jenkins;
kjenkins@xiliotx.com

ABSTRACT

Introduction The clinical benefit of the anti-CTLA-4 monoclonal antibody (mAb) ipilimumab has been well established but limited by immune-related adverse events, especially when ipilimumab is used in combination with anti-PD-(L)1 mAb therapy. To overcome these limitations, we have developed XTX101, a tumor-activated, Fc-enhanced anti-CTLA-4 mAb.

Methods XTX101 consists of an anti-human CTLA-4 mAb covalently linked to masking peptides that block the complementarity-determining regions, thereby minimizing the mAb binding to CTLA-4. The masking peptides are designed to be released by proteases that are typically dysregulated within the tumor microenvironment (TME), resulting in activation of XTX101 intratumorally. Mutations within the Fc region of XTX101 were included to enhance affinity for FcγRIII, which is expected to enhance potency through antibody-dependent cellular cytotoxicity.

Results Biophysical, biochemical, and cell-based assays demonstrate that the function of XTX101 depends on proteolytic activation. In human CTLA-4 transgenic mice, XTX101 monotherapy demonstrated significant tumor growth inhibition (TGI) including complete responses, increased intratumoral CD8+ T cells, and regulatory T cell depletion within the TME while maintaining minimal pharmacodynamic effects in the periphery. XTX101 in combination with anti-PD-1 mAb treatment resulted in significant TGI and was well tolerated in mice. XTX101 was activated in primary human tumors across a range of tumor types including melanoma, renal cell carcinoma, colon cancer and lung cancer in an ex vivo assay system.

Conclusions These data demonstrate that XTX101 retains the full potency of an Fc-enhanced CTLA-4 antagonist within the TME while minimizing the activity in non-tumor tissue, supporting the further evaluation of XTX101 in clinical studies.

WHAT IS ALREADY KNOWN ON THIS TOPIC

- ⇒ In the clinic, efficacy of CTLA-4 antagonists such as ipilimumab is frequently accompanied by immune-related adverse events that limit clinical use.
- ⇒ Endogenous dysregulation of proteases within the tumor microenvironment enables intratumoral activation of prodrugs, thereby potentiating localized activity to the tumor while minimizing systemic activity in the periphery.

WHAT THIS STUDY ADDS

- ⇒ We disclose here the discovery efforts to generate XTX101, a tumor-activatable, Fc-enhanced anti-CTLA-4 mAb, including identification of a high-affinity anti-CTLA-4 monoclonal antibody, biopanning to identify CDR masks, and incorporation of mutations within the Fc to enhance affinity for FcγRIII.
- ⇒ Preclinical research includes in vitro studies validating protease-dependent activity, in vivo murine tumor models demonstrating antitumor activity and tumor-specific function, and activation of XTX101 prodrug via human tumor samples in an ex vivo assay system.

HOW THIS STUDY MIGHT AFFECT RESEARCH, PRACTICE OR POLICY

- ⇒ The preclinical demonstration of superior antitumor activity and intratumoral-specific pharmacodynamics of XTX101 in murine tumor models compared with ipilimumab and ex vivo activation via human tumor samples support the hypothesis of tumor-specific activation of a highly potent biologic; these findings warrant further evaluation in an ongoing clinical trial (NCT04896697).

BACKGROUND

A new era of cancer therapeutics began in 2011 with the U.S. Food and Drug Administration (FDA) approval of the first immune

checkpoint inhibitor, ipilimumab, for the treatment of patients with late-stage melanoma. Ipilimumab targets CTLA-4, a protein responsible for T cell regulation.¹ CTLA-4 is a T cell receptor of the Ig superfamily containing an extracellular single variable-like domain and shares structural homology to the T cell activation receptor CD28.^{2,3} CTLA-4 and CD28 competitively bind to co-stimulatory receptors CD80 and CD86 displayed on antigen-presenting cells, although CTLA-4 has ~10-fold to 20-fold higher affinity for these molecules.⁴ Despite the structural homology and shared ligands, CD28 and CTLA-4 have opposing effects on T cells' response to stimulation.⁵ The engagement of CD28 with CD80/86 results in T cell activation, whereas CTLA-4 interaction with CD80/86 leads to T cell anergy.⁶ Blocking the CTLA-4:CD80/86 interaction with an antagonistic anti-CTLA-4 mAb results in antitumor response in multiple preclinical mouse tumor models (reviewed in previous work⁷).

In clinical studies, the CTLA-4 antagonist, ipilimumab, has demonstrated meaningful efficacy when employed as monotherapy or in combination with anti-PD-(L)1 antagonists across numerous cancer indications including melanoma, hepatocellular carcinoma, non-small cell lung cancer (NSCLC), renal cell carcinoma (RCC), microsatellite instability high colorectal cancer, and malignant pleural mesothelioma. While ipilimumab treatment demonstrated a significant improvement in overall survival, treated patients also demonstrated significant on-target/off-tumor toxicities.^{1,8-11} In a phase III clinical trial of ipilimumab in patients with melanoma, the median overall survival was improved at the 10 mg/kg dose compared with the 3 mg/kg dose (15.7 months vs 11.5 months, respectively), demonstrating that a higher dose of ipilimumab resulted in a higher survival of patients. However, the corresponding increase in Gr. 3/4 immune-related adverse events (irAEs) at the 10 mg/kg dose resulted in unacceptable toxicity for many patients.¹²

Beyond CTLA-4 blockade and inhibition of CD80/86 ligand binding by ipilimumab, further studies indicate a possible secondary mechanism of anti-CTLA-4 mAbs. Interaction with NK cells and macrophages also leads to antibody-dependent cell-mediated cytotoxicity (ADCC) and thus depletion of regulatory T cells (Tregs).^{13,14} In vitro studies have shown a correlation between anti-CTLA-4 mAb affinity for FcγRIII and ADCC activity induced by the anti-CTLA-4 mAb.¹⁵ Furthermore, altering the Fc and reducing ADCC activity of an anti-CTLA-4 mAb resulted in suboptimal Treg depletion and diminished potency in multiple mouse tumor models.¹⁵⁻¹⁷ This observation is borne out in the clinic: improved clinical response to ipilimumab observed in patients with advanced melanoma has been linked with high load of somatic mutations and the presence of germline polymorphism FcγRIIIa V158F.^{15,18} In a recent early phase trial, botensilimab, a CTLA-4 mAb with enhanced binding to activating Fc receptors, in combination with anti-PD-1 mAb balstilimab demonstrated an increase in the durable objective response rate in heavily pretreated

patients with microsatellite stable colorectal cancer (MSS CRC).¹⁹ These results suggest that anti-CTLA-4 mAbs armed with enhanced ADCC capacity through increased affinity for FcγRIII could improve clinical responses in patients. Such mAbs are now being tested in the clinic and have shown promise, but their use may remain limited due to toxicities resulting from systemic CTLA-4 antagonism.^{20,21} We hypothesize that localizing the activity of an anti-CTLA-4 mAb with enhanced ADCC capacity intratumorally will result in Treg depletion and an increase in CD8+T cells in the tumor while minimizing the activation of T cells in non-tumor tissue, which is generally associated with toxicities from constitutively active CTLA-4 antagonists.

To this end, we have generated XTX101, a tumor-activated, Fc-enhanced anti-CTLA-4 mAb. XTX101 has multiple components designed to increase its therapeutic index: (1) a humanized mAb with high affinity to human CTLA-4; (2) mutations within the Fc region to enhance binding to FcγR; (3) a masking peptide with low micromolar affinity and a fast off-rate for the complementarity-determining regions (CDR) of the mAb; and (4) a matrix metalloproteinases (MMP)-sensitive linker connecting the masking peptide to the mAb. In its intact form, XTX101 is a prodrug with minimal binding to CTLA-4. When XTX101 enters the tumor microenvironment (TME), the MMP-sensitive linker is cleaved by proteases that are naturally upregulated and activated within the tumor tissue, thereby freeing the peptide mask and activating the mAb. Activity of XTX101 relies on the natural phenomenon of protease dysregulation within the TME. Dysregulation of proteases resulting in an increase in intratumoral proteolytic activity is generally considered pro-tumorigenic, as proteases can regulate tumor growth, inflammation, angiogenesis, tissue invasion, and metastasis.²²⁻²⁵ This dysregulation of proteases in the TME has recently garnered interest as a means for activating prodrugs intratumorally. For example, the gelatinases MMP-2 and MMP-9 have been identified as compelling proteases for intratumoral activation of prodrugs due to the extensive characterization of their substrate preferences, their role in tumor biology, and the elaborate inhibitory control system regulating their activity in non-tumor tissue.²⁶⁻³¹

In this report, we evaluated the relationship between XTX101 activation by proteases, both recombinant and TME-derived, and function. In vitro studies used recombinant MMPs for XTX101 activation, and function was compared with unmasked control mAb XTX100. Syngeneic mouse tumor models evaluated the activation of XTX101 by tumors in vivo and the downstream pharmacodynamics, including depletion of Tregs. Finally, fresh human tumor samples were used to assess the tumor activation of XTX101 in an ex vivo assay system. We report here the preclinical proof-of-concept of tumor-activated, Fc-enhanced XTX101 that has the potential to enhance anti-CTLA-4 mAb antitumor activity with an improved tolerability profile.

METHODS

Protein expression and purification

ATX110, XTX100, XTX101, ipilimumab-analog, and isotype control mAb were produced at Xilio Therapeutics. ATX110 was generated using rat hybridoma technology and subsequently humanized. Mutations S239D and I332E³² were incorporated in the Fc region to generate XTX100, XTX101, and isotype mAb. XTX101 consists of humanized anti-CTLA-4 mAb XTX100 linked to a masking peptide by a linker containing an MMP substrate.²⁶ The masking peptide was discovered by Xilio Therapeutics. For additional details on designs, please refer to patent application #WO2020139920A2. Ipilimumab-analog was produced as the amino acid sequence of ipilimumab (CAS 477202-00-9) with a K448 deletion on the heavy chain. Proteins were expressed from transient transfection in human embryonic kidney (HEK293) cells obtained from the National Research Council or ExpiCHO (Thermo Fisher Scientific). Conditioned media was harvested 5–7 days after the transfection, centrifuged, and filtered with 0.2 μ m filters. Filtered supernatants were subjected to affinity chromatography purification using protein A resin columns (GE Healthcare) or protein G resin (GenScript). Proteins were eluted from affinity columns, brought to pH 5.5 with acetate buffer, and stored at -80°C .

Biopanning with phage display peptide library

The XTX100 mAb was captured on ProteinG Magnetic Beads (88847, Thermo Fisher Scientific) at room temperature (RT) for 30 min. Unbound mAb was removed by washing with TBS, and XTX100-immobilized beads were blocked with TBS+milk. Beads were incubated with a peptide phage display library displaying cyclic 7-mer peptides at RT for 30 min, followed by vigorous washing with tris-buffered saline + 0.1% Tween (TBS-T). Bound phage was eluted with 0.2 M glycine pH 2.2, added to a pH-neutralization solution, and amplified by infecting into *Escherichia coli* K12 ER2738 (E4104, New England Biolabs). Two subsequent rounds of biopanning were performed. Individual clones were isolated from the final pool and analyzed by DNA sequencing and by ELISA. ELISA of individual phage clones was performed according to manufacturer's protocol (E8120S, New England Biolabs). Briefly, wells of a 96-well plate (44-2404-21, Thermo Fisher Scientific) were coated with 100 μ L of phosphate-buffered saline (PBS), XTX100, or isotype antibody, each mAb at 1 mg/mL in PBS. Plate was covered and incubated overnight at 4°C . 5% dry milk in TBS was used as blocking solution. Individual phage clone samples in assay buffer (TBS-Tween (TBS-T)+5% dry milk) were applied to the washed plate. Bound phage was detected using HRP-linked anti-M13 antibody (GE27-9421-01, GE Healthcare). Addition of peroxidase substrate ABTS solution (A1888, Sigma-Aldrich) was added for measurement of optical density at 415 nm after 13 min.

Surface plasmon resonance (SPR) analyses

Peptides binding to Fab

Peptides were synthesized by GenScript. XTX100-Fab was prepared as discussed above and diluted to 25 μ g/mL in 50 mM sodium acetate pH 5.0. The diluted XTX100-Fab was then immobilized to a CM5 sensor chip via amine coupling (BR100050, Cytiva). Peptides were flowed over the chip at concentrations of 1–100 μ M at a temperature of 37°C .

mAb binding to hCTLA-4

Recombinant human CTLA-4Fc (7268-CT-100, R&D Systems) was diluted to 30 μ g/mL in 50 mM sodium acetate pH 5.0. The diluted antigen was then immobilized onto a carboxymethyl dextran-coated SPR sensor chip (13206066, Reichert Technologies) via amine coupling (BR100050, Cytiva). Analytes XTX100, XTX101, and pre-activated XTX101 were flowed over the chip at concentrations of 2–32 nM at 25°C .

mAb binding to Fc γ RIIIa

Recombinant human Fc γ RIIIa (4325-FC-050, R&D Systems) was diluted to 30 μ g/mL in 50 mM sodium acetate pH 5.0. The diluted Fc γ R was then immobilized onto a carboxymethyl dextran-coated SPR sensor chip (13206066, Reichert Technologies) via amine coupling (BR100050, Cytiva). ATX110 was flowed over the chip at concentrations of 125 nM to 2 μ M. XTX100 and pre-activated XTX101 were flowed over the chip at concentrations of 1–16 nM at a temperature of 25°C .

Fab binding to hCTLA-4

XTX100-Fab, ipilimumab-analog-Fab, and Yervoy-Fab (IgG—NDC 00003-2327-1, Myoderm) prepared as discussed above and immobilized onto a carboxymethyl dextran-coated SPR sensor chip (13206066, Reichert Technologies) via amine coupling (BR100050, Cytiva). Human CTLA-4 (7268-CT-100, R&D Systems) flowed over the chip at concentrations of 0.781–100 nM at a temperature of 37°C .

The k_a and k_d were determined using TraceDrawer or Biacore T100 evaluation software and used to calculate the K_d for each antigen-antibody interaction.

Crystal structures of peptide: Fab complexes

XTX100-Fab was produced from CHO cells and purified with affinity (protein G resin, GenScript) and size-exclusion chromatography (Superdex 75 Increase 10/300 GL, 29148721, Cytiva Lifesciences) in crystal buffer (10 mM Tris-HCl pH 8.0, 25 mM NaCl, 1 mM EDTA).

XTX100-Fab+CPGKGLPSC complex

Purified XTX100-Fab was crystallized using the hanging drop vapor diffusion method over a reservoir containing 0.5 mL of 0.2 M ammonium citrate pH 7.0 and 23% PEG 3350. Hanging drops were prepared at 60 μ M XTX100-Fab with 10x molar excess (600 μ M) peptide and mixed 1:1 with reservoir solution.

Crystals were harvested in cryoprotectant (1:1 mix of 35% (w/v) meso-erythritol and reservoir solution) and mounted under cryo-conditions on a Rigaku MicroMax007-HF rotating anode diffractometer with a Rigaku RAXIS IV++ detector. A native dataset was collected at 1.5418 Å at 100 K and processed using X-ray Detector Software (XDS), resulting in a 98.8% complete dataset to 3.0 Å. The complex crystallized in space group $P2_12_12_1$ (unit cell dimensions 72.1 Å, 202.8 Å, 224.6 Å, 90°, 90°, 90°) with six complexes per asymmetric unit.

The initial solution was obtained via molecular replacement using Phaser in the Phenix suite with previously determined XTX100-Fab as a search model as a search model. This solution was then subjected to several cycles of manual building followed by refinement using phenix.refine. Data collection and refinement statistics are listed in online supplemental table 2.

XTX100-Fab+CPFPALC complex

Purified XTX100-Fab was crystallized using the hanging drop vapor diffusion method over a reservoir containing 0.5 mL of 0.2 M ammonium citrate dibasic pH 5.0 with 20% PEG 3350. Hanging drops were prepared at 60 μM XTX100-Fab with 10x molar excess (600 μM) peptide and mixed 1:1 with reservoir solution.

Crystals were harvested in cryoprotectant (1:1 mix of 35% (w/v) meso-erythritol and reservoir solution) and mounted under cryo-conditions on a Rigaku MicroMax007-HF rotating anode diffractometer with a Rigaku RAXIS IV++ detector. A native dataset was collected at 1.5418 Å at 100 K and processed using XDS, resulting in a 96.6% complete dataset to 2.4 Å resolution. The complex crystallized in space group I21 (unit cell dimensions 63.38 Å, 57.9 Å, 116.267 Å, 90°, 95.6°, 90°) with one complex per asymmetric unit.

The initial solution was obtained via molecular replacement using Phaser in the Phenix suite with previously determined XTX100-Fab as a search model. This solution was then subjected to several cycles of manual building followed by refinement using phenix.refine. Data collection and refinement statistics are listed in online supplemental table 2.

In vitro activation of XTX101 with recombinant enzymes

Recombinant human proteases MMP-1 (901-MP-010), MMP-2 (902-MP-010), MMP-7 (907-MP-010), MMP-9 (911-MP-010), and MMP-10 (910-MP-010) were purchased from R&D Systems. All MMPs except MMP-14 were activated by diluting to 0.22 mg/mL in MMP buffer (150 mM NaCl; 50 mM Tris, pH 7.5; 10 mM CaCl₂; filtered) and incubating with equal volume of 1 mM 4-aminophenylmercuric acetate (A9563, Sigma-Aldrich) at 37°C for 2 hours. MMP-14 (918-MP-010, R&D Systems) was activated by diluting to 0.16 mg/mL in MMP buffer and incubating with equal volume of 3.44 ng/μL recombinant human furin (R&D Systems) at 37°C for 2 hours. For experiments in which activated XTX101+MMP was used, XTX101 was incubated with activated MMP-9 for

16–18 hours at 37°C, then frozen for later use. Intact XTX101 was also incubated without protease at 37°C, then frozen for later use as a control.

Determination of the catalytic efficiency for XTX101 activation with recombinant human MMPs

The catalytic efficiency (k_{cat}/K_m) of recombinant human MMP-1, MMP-2, MMP-7 to MMP-9, MMP-10, or MMP-14 to activate XTX101 was assessed by cleavage time-course assay.

To initiate a cleavage reaction, 20 nM active MMP was combined with 2 μM XTX101 in assay buffer (50 mM Tris-HCl, 10 mM CaCl₂, 150 mM NaCl, 0.05% Brij35, pH 7.5), and incubated at 37°C. Aliquots were removed and quenched with 50 mM EDTA over a time-course spanning 47 hours. Following that, the quenched reaction aliquot was extracted and analyzed by reducing CE-SDS technology, according to the manufacturer's protocol (LabChip GXII Touch HT, PerkinElmer). Chromatogram peaks identified as intact light chain (LC) and activated LC were integrated and used to quantify the percent activation using the following formula:

$$\% \text{ activation} = (\text{intact LC} / (\text{intact LC} + \text{activated LC})) \times 100\%$$

The result was plotted against time in GraphPad Prism and fit to one-phase association model. The derived first-order constant K was then divided by MMP concentration to yield catalytic efficiency, as defined by one-step enzymatic reaction mechanism.³³

CTLA-4 antigen ELISA

A 96-well plate was coated with recombinant human CTLA-4 (7268-CT-100, R&D Systems) 1 μg/mL solution diluted in PBS. Plates were covered and stored at 4°C overnight. The next day, the plates were washed with TBS-T, three times with 200 μL per well. Blocking solution (PBS+1% bovine serum albumin (BSA)) was added to the plates and stored at 4°C for >2 hours. After blocking, plates were washed with TBS-T. Test articles were serially diluted in assay buffer (PBS-Tween+1% BSA) and added to the plate in duplicate. Plates were covered and incubated at RT with shaking for 1 hour. Plates were washed, and detection antibody horseradish peroxidase (HRP)-conjugated anti-KappaLC mAb (ab79115, Abcam) was added. Plates were covered and incubated at RT with shaking for 1 hour. Plates were washed, and HRP-chemiluminescent substrate (37069, Thermo Fisher) was added. Plates were covered and incubated at RT for 5 min, protected from light. After incubation, chemiluminescence was measured and data were fit by non-linear regression analysis by GraphPad Prism.

CD80/86 competition ELISA

A 96-well plate was coated with recombinant human CTLA-4 (7268-CT-100, R&D Systems) and blocked as above. Serial dilutions of test articles were added to the washed ELISA plates followed by addition of a 2.6 μg/mL solution of recombinant human CD80 or CD86 (9050-B1-100 or 9090-B2-100, R&D Systems). Plates were

washed and HRP-conjugated anti-His antibody (652504, BioLegend) was added to the plate. Plates were washed followed by incubation with chemiluminescent substrate (37069, Thermo Fisher Scientific). After incubation, chemiluminescence was measured in Light Units by a plate reader. Data were fit by non-linear regression analysis. IC_{50} values represent the concentration at which 50% of maximum CD80 or CD86 was bound to CTLA-4.

ADCC reporter bioassay

The ADCC reporter bioassay was performed according to the protocol provided by vendor (ADCC Reporter Bioassay Core Kit TM383, Promega). Briefly, Raji-CTLA-4 target cells (raji-hctla4, Invivogen) were incubated with Jurkat-FcγRIIIa effector cells (Promega) at 1:1 ratio in the presence of serial dilutions of XTX100 or XTX101 (1 to 30,000 ng/mL, final concentrations). After 6 hours, NFAT-induced Luciferase production was measured by activation of luminescent substrate. Non-linear regressions were generated by GraphPad Prism, and the $EC_{50} \pm SE$ for each test article was reported.

Staphylococcal enterotoxin B (SEB) assay

Peripheral blood mononuclear cells (PBMCs) from pooled healthy human donors (BioIVT) were purchased and stored $\leq -150^{\circ}C$ in liquid nitrogen until use. Test articles were serially diluted in pre-warmed medium: RPMI 1640 (21870-076, Thermo Fisher Scientific), 10% heat-inactivated FBS (A38400-01, Thermo Fisher Scientific), 10 mM HEPES (15630-080, Thermo Fisher Scientific), 1% NEAA (1140-050, Gibco), 1 mM sodium-pyruvate (11360-070 Thermo Fisher Scientific), and 1x L-glutamine (25030-081, Gibco). Diluted test articles were applied to 96-well plate in triplicate. SEB (BT202, Toxin Technology) solution was prepared in pre-warmed medium at 255 ng/mL and applied to the plate. PBMCs were thawed, washed twice with pre-warmed medium, adjusted to 1×10^6 cells/mL, and added to 96-well plate. The plates were incubated at $37^{\circ}C$ at 5% CO_2 . After 5 days, the supernatants were harvested, and IL-2 in the supernatant was measured by ELISA according to manufacturer's protocol (431804, BioLegend).

Cell lines

Murine colon carcinoma cell line MC38 was grown and maintained by Biocytogen Boston Corp (Wakefield, Massachusetts, USA). Murine bladder carcinoma cell line MB49 was obtained from EMD Millipore and were maintained at Xilio Therapeutics. Both cell lines were in culture less than 2 weeks prior to inoculation. MC38 cells were cultured as monolayer culture in DMEM (Gibco, 10569-010) supplemented with 10% FBS (HyClone, SH30088.03), 0.1 mM non-essential amino acids (Gibco, 11140050), and 10 mM HEPES (Gibco, 15630080). MB49 cells were cultured in RPMI 1640 (Gibco, 11875) supplemented with 10% FBS (ATCC, 30-2020), 0.1 mM non-essential amino acids (Life Technologies, 11140-050), and 1 mM sodium pyruvate (Life Technologies, 113600-070).

Cells were incubated in a humidified incubator at $37^{\circ}C$ in an atmosphere with 5% CO_2 . The tumor cells were routinely subcultured by trypsin-EDTA treatment twice a week. The cells in an exponential growth phase were harvested, washed with PBS, and counted for inoculation.

Mice, tumor inoculations, and dosing

The care and use of animals were conducted in accordance with the regulations of the Association for Assessment and Accreditation of Laboratory Animal Care (AAALAC). All mice were purchased from Biocytogen. Female, 7–10 week old B-hCTLA4 (C57BL/6-*CTLA4^{fl}m1(CTLA4)*/Bcgen) mice were subcutaneously injected with 1×10^6 MB49 and monitored for tumor growth in a non-blinded experiment. Tumor width and length were measured using dial calipers, and tumor volumes were calculated by the formula: $Tumor\ volume = l * w^2 / 2$, where l =length and w =width, in mm. For the tumor growth inhibition (TGI) cohorts, mice were randomized into treatment groups ($n=8$ mice per group) when tumor volume reached $\sim 150\text{ mm}^3$. For the tumor pharmacodynamics cohort, mice were randomized into treatment groups ($n=5$ mice) when tumor volume reached $\sim 350\text{ mm}^3$. MB49 tumor-bearing mice were given a single, 200 μ L intravenous bolus injection of 1, 3 or 10 mg/kg of isotype control, ipilimumab-analog, XTX100, or XTX101. After injection, tumor volumes were measured twice a week. Mice were monitored for a total of 67 days after initiation of treatments. Animals were removed from the study and euthanized if tumor volume reached 2000 mm^3 or bodyweight loss was greater than 20%. On day 68, mice with no palpable evidence of tumors were considered complete responders and were subsequently re-challenged with a SC injection of 1×10^6 MB49 cells on the opposite flank. As a control, five non-treated (naïve) mice were also inoculated with MB49 cells in the same manner.

In the anti-PD-1 combination study, female, 13–14 week old B-hCTLA4 (C57BL/6-*Ctla4^{fl}m1(CTLA4)*/Bcgen/Bcgen) mice were injected SC with 5×10^5 MC38 cells. Mice were randomized into treatment groups ($n=8$ mice) when tumor volume reached $\sim 150\text{ mm}^3$. MC38 tumor-bearing mice were given a single, 100 μ L intravenous bolus injection of 0.3 mg/kg of isotype control or XTX101 on day 0 and/or three 100 μ L intraperitoneal injections of 10 mg/kg of anti-murine PD-1 mAb clone RMP1-14 (BP0146, BioXCell) Q3D beginning on day 0. Mice were monitored for a total of 55 days after initiation of treatments. Animals were removed from the study and euthanized if tumor volume reached 2000 mm^3 or bodyweight loss was greater than 20%.

Immunophenotyping using flow cytometry

For immunophenotypic analysis of peripheral blood from TGI cohort, samples were collected from the submandibular vein on day 5 followed by lysis of red blood cells. In the tumor pharmacodynamics cohort, mice were euthanized on day 7 by CO_2 asphyxiation, and spleens and tumors were harvested. Cell suspensions were prepared

from spleens by mechanical disruption followed by lysis of red blood cells. Tumor cell suspensions were prepared by combining mechanical dissociation with enzymatic degradation of the extracellular matrix to achieve single-cell suspensions. The tumor tissues were enzymatically digested using Miltenyi Tumor Dissociation Kit (130-096-730, Miltenyi Biotech) and the gentleMACS Dissociator was used for the mechanical dissociation steps. Following tumor digestion, debris was separated by sedimentation, and suspensions were passed through a 40 µm nylon cell strainer. Single cell suspensions were incubated with antibody cocktails for cell surface staining. Intercellular staining was performed using the fixation/permeabilization staining buffer set (00-5523-00, eBioscience). The optimal concentration for each antibody was predetermined by titration. Flow cytometry antibodies used were anti-mouse CD3 (100246, BioLegend), CD4 (100538, BioLegend), CD25 (102042, BioLegend), CD8 (100730, BioLegend), CD45 (103149, BioLegend), ICOS (313530, BioLegend), Foxp3 (12-5773-82, eBioscience), and Ki-67 (11-5698-82, eBioscience).

The gating strategy applied for the analysis was as follows: a parental gate was created around the lymphocyte population as identified by low forward scatter and low side scatter characteristics. From the lymphocyte gate, subpopulations of immune cells were identified on dot plots: leukocytes (CD45⁺), helper T cells (CD3⁺ CD4⁺), cytotoxic T lymphocytes (CD3⁺ CD8⁺), and regulatory T cells (CD3⁺ CD4⁺ FOXP3⁺ CD25⁺).

Ex vivo assay with fresh human tumor samples

Preparation of tumor conditioned media (TCM)

Tumor tissues were obtained from Cooperative Human Tissue Network divisions (CHTN) and were shipped overnight at 4°C after surgical resection. On receipt, tissues were cut with scalpels into small 2–3 mm pieces and then transferred into a C-Tube (130-093-237, Miltenyi) containing 5 mL of 1% penicillin-streptomycin (15070-063, Gibco) in RPMI 1640 (11875-093, Gibco) for homogenization using the GentleMACS program 'h_tumor_02'. This process was performed three consecutive times, with a 5-minute incubation at RT in between each cycle.

The tumor tissue homogenate was collected and 1% P/S-RPMI was added, according to tumor weight: 6 mL 1% P/S-RPMI per 100 mg tumor. The homogenate was then distributed in a 6-well plate and incubated for 1, 2, 3, or 4 days, at 37°C and 5% CO₂. After incubation, conditioned media was collected and centrifuged once at 475×g for 10 min, followed by two times at 3200×g for 20 min. The supernatant was then filtrated using 0.22 µm filters and used immediately as TCM for the ex vivo activation assay.

Ex vivo activation assay

XTX101 (30 µg) was incubated in 200 µL TCM. As controls, 30 µg of XTX101 and XTX100 were incubated in 200 µL fresh RPMI media. Samples were incubated for 2, 3 or 4 days at 37°C and 5% CO₂ under agitation

(300 rpm). Following incubation, samples were applied to a CTLA-4 binding ELISA for assessment of % activation.

The percent (%) of activation was calculated based on the activity of XTX101 incubated in TCM compared with that of control sample XTX101 in incubated in fresh RPMI media and unmasked mAb XTX100 using the following formula:

% of activation =

$$100\% * K_D \text{XTX100} * \frac{K_D \text{XTX101 in TCM} - K_D \text{XTX101 in RPMI}}{K_D \text{XTX101 in TCM} (K_D \text{XTX100} - K_D \text{XTX101 in RPMI})}$$

where the K_D was determined by the CTLA-4 binding ELISA. A 1% activation cut-off, the lower limit of quantification of activated XTX101 by ELISA, was used to determine the proportion of tumor supernatant samples that were able to activate XTX101. Therefore, activation above or equal to this threshold was scored as positive evidence of the ability of proteases from the tumor sample to activate XTX101.

Data representation and statistical analysis

For in vitro activity assays, background signal was subtracted from the data in Excel and exported to GraphPad Prism V.8 for data analyses using a non-linear sigmoidal, 4PL curve fit model without constraints. All in vitro assays have been repeated at least twice.

Tumor growth data were analyzed in GraphPad by plotting tumor growth curves with the mean tumor volume of each group on the X axis and the time point of each measurement on the Y axis; the SEM was represented with error bars. Differences between treatment groups and the isotype control group were calculated as mean %TGI using the formula: %TGI = (1-T/C)×100%, where T is the treatment group and C is the isotype control group.

For murine immunophenotyping studies, FlowJo V.10 software was used to analyze the flow cytometry data prior to exportation for graphing and statistical analysis in GraphPad.

Repeated measures two-way analysis of variance (ANOVA) test with Bonferroni's post hoc pairwise comparison tests were performed to determine the statistical significance of observed differences in tumor volumes. Kaplan-Meier curves were used to estimate the survival function of the treated mice. Statistical significance of observed differences between study groups in survival were measured using the log-rank (Mantel-Cox) test with Bonferroni's multiple comparison correction. A one-way ANOVA test with Bonferroni's post hoc pairwise comparison tests was performed to determine the statistical significance of the observed differences in immunophenotypic changes. All statistical tests were performed in GraphPad Prism.

Data availability

The atomic coordinates have been deposited to the PDB under 8G2M and 8G8N. All other data generated in this study are available within the article and online supplemental data files. We used the Animal Research:

Reporting of In Vivo Experiments (ARRIVE) checklist when writing our report.³⁴

RESULTS

Discovery of conditionally activated anti-CTLA-4 mAb XTX101

XTX101, a tumor-activated anti-CTLA-4 mAb with enhanced potency, was designed to enhance the therapeutic index of CTLA-4 antagonism by decreasing the toxicity associated with systemically active ipilimumab. ATX110 was initially identified using rat hybridoma technology followed by humanization. ATX110 had a higher affinity to CTLA-4 than both clinical-grade ipilimumab (Yervoy) and internally produced ipilimumab-analog, as determined by SPR (online supplemental figure 1). ATX110 did not bind to CD28, a costimulatory T cell receptor containing high degree of sequence and structural homology with CTLA-4 (data not shown).³⁵ ATX110 was modified by including mutations S239D/I332E to the Fc region (herein referred to as XTX100) to enhance affinity for human FcγRIIIa.³² The affinity of XTX100 for human FcγRIIIa was 8.42 nM, a 17-fold increase from the ATX110 mAb without the Fc enhancement mutations (online supplemental figure 2).

To identify peptides that bind to the CDRs of XTX100 and serve as masking moiety, a library of phage displaying cyclic 7-mer peptides was used for biopanning. After the third round of biopanning against XTX100, 10 phage clones were isolated and peptide sequences were identified (online supplemental table 1). Seven of these clones were found to be unique. To assess the selective binding of phage clones to XTX100, individual phage clones were amplified and analyzed for binding by ELISA (figure 1A). Phage clones producing a positive ELISA signal for selective XTX100 binding were clones 1/2/6 (CPGKGLPSC), 3 (CPFPAKILC), 4 (CTKPAKALC), 5 (CIHAPYAKC), 7 (CPFPALELC), 8 (CPAKIGQEC), and 10 (CKHAPYALC). Peptides from identified clones were synthesized, and two peptides (CPGKGLPSC and CPFPALELC) had low micromolar affinity with a fast dissociation rate for XTX100, as determined by SPR (figure 1B,C).

The complex of either peptide with XTX100 was elucidated by X-ray crystallography (figure 2). In one instance, XTX100 Fab was co-crystallized with peptide CPGKGLPSC (figure 2A). The structural data identified Lys4_{peptide} as a critical residue, as it facilitated interactions with residues in CDR2 of the Fab heavy chain (HC) through hydrogen bonds and/or salt bridges with Asp52_{HC} and Glu54_{HC}. PDBEPIA also predicted a potential hydrogen bond between Cys1_{peptide}:Arg50_{HC}. In a second instance, XTX100 Fab was co-crystallized with peptide CPFPALELC (figure 2B). This structure exhibited interactions between the Glu7_{peptide} and CDR3 of HC via hydrogen bond and salt bridge with Tyr104_{HC} and Arg99_{HC}, respectively. Other interactions from this complex included hydrogen bonds between Phe3_{peptide}:Arg50_{HC} and a hydrogen bond and/or salt bridge between Cys1_{peptide}:Asp59_{HC}. Both peptides contained an intramolecular disulfide bond between

Cys1 and Cys9. A superposition of both crystal structures confirmed an overlap of binding sites for both peptides and interactions with the CDRs of the heavy chain (figure 2C). The totality of these data suggests either peptide could serve as a suitable mask for the design of XTX101.

XTX101 in vitro activity and function is reliant on proteolytic activation

The crystal structure subsequently guided the design of XTX101 (figure 3A). A linker containing an MMP-sensitive substrate connects the peptide to the light chain of XTX100, so that the peptide blocks the CDR:CTLA-4 interaction (figure 3A, middle). Proteolytic activation of the MMP-sensitive linker severs the covalent bond between the peptide to the mAb, and the CDRs are subsequently liberated from the peptide mask and therefore able to bind CTLA-4 (figure 3A, right). In vitro studies with recombinant proteases demonstrated proteolytic activation of XTX101 by multiple human MMPs with catalytic efficiencies ranging from 1.2×10^3 to $4.6 \times 10^4 \text{ M}^{-1} \text{ s}^{-1}$ (online supplemental figures 3 and 4, online supplemental table 3).

The relative binding of intact XTX101, proteolytically activated XTX101 (XTX101+MMP), and unmasked XTX100 to human CTLA-4 was measured. By ELISA, XTX100 bound human CTLA-4 with K_D value of 0.16 nM, and XTX101+MMP similarly bound human CTLA-4 with K_D value of 0.24 nM (figure 3B). As expected, intact XTX101 bound human CTLA-4 with a K_D value of 19.4 nM, a 121-fold and 81-fold reduction in binding compared with XTX100 and activated XTX101, respectively. Reduced binding of intact XTX101 to CTLA-4 was confirmed by SPR experiments (figure 3C). Analytes XTX100 and XTX101+MMP demonstrated 91 and 127 pM affinities, respectively, for immobilized human CTLA-4, whereas intact XTX101 had no measurable affinity for CTLA-4 over the concentration range tested. These results indicate activated XTX101 and XTX100 bound to human CTLA-4 at comparable affinities, and intact XTX101 had a significant reduction in binding to CTLA-4.

A fundamental mechanism of action for CTLA-4 antagonists such as ipilimumab is the inhibition of CTLA-4 binding to its ligands, CD80 and CD86.³⁶ Activated XTX101 exhibited potent inhibition of CTLA-4 binding to CD80 and CD86 in a competition ELISA, whereas the inhibition of CD80 and CD86 ligand binding to intact XTX101 was reduced by 120-fold and 81-fold, respectively (figure 4A,B). Comparable results were observed in an ADCC bioassay, a two-cell system in which response is dependent on mAb binding to CTLA-4 expressing target cells. In this experiment, activated XTX101 exhibited a response similar to unmasked control XTX100 (figure 4C). In contrast, the signal from intact XTX101 was greatly reduced, such that an accurate EC_{50} could not be calculated. Function of XTX101 was further evaluated in human PBMCs stimulated with the superantigen

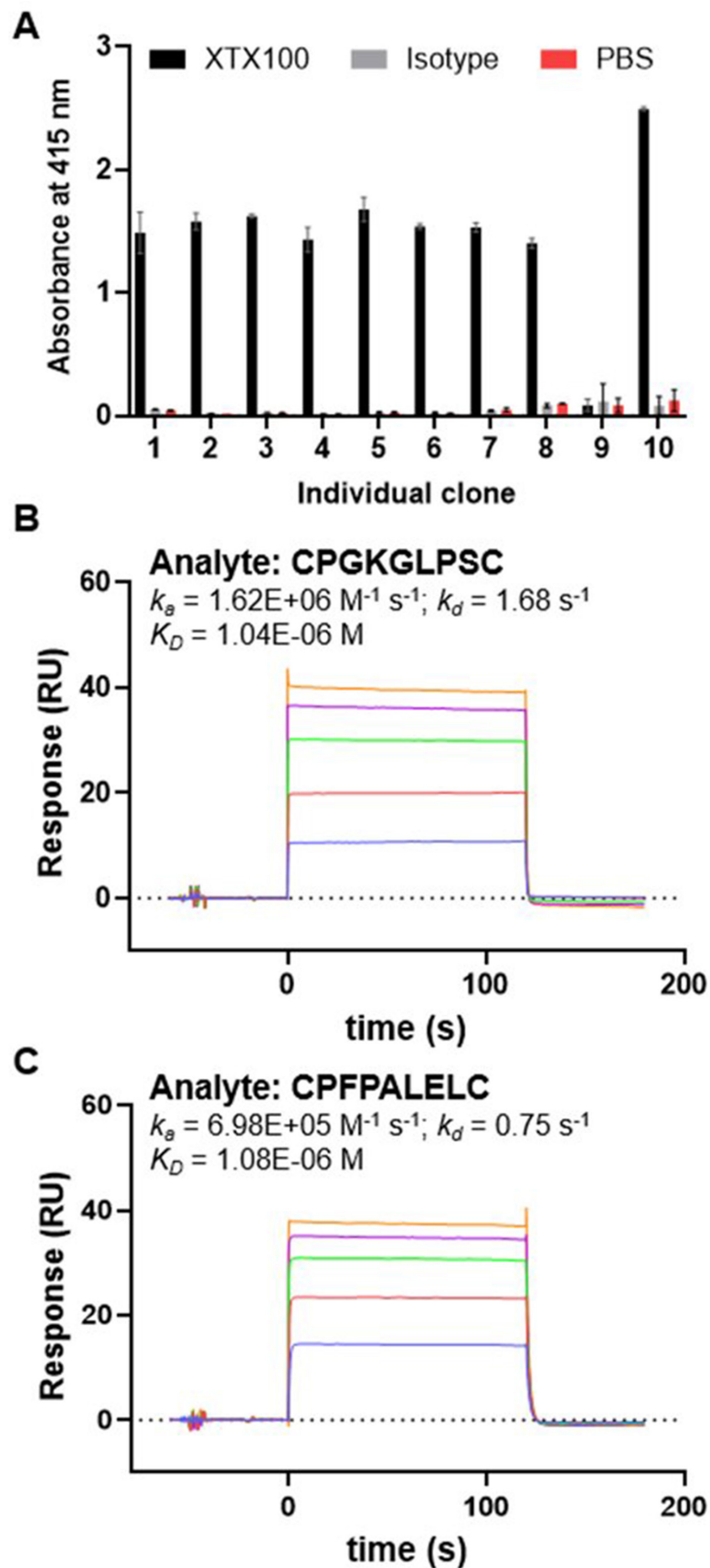


Figure 1 Identification of peptide mask. (A) ELISA results of individual phage clones binding to XTX100 (black), isotype mAb (gray), or phosphate-buffered saline (PBS) only (red). (B, C) Reference subtracted surface plasmon resonance sensorgrams of peptides CPGKGLPSC (B) and CFPFALELC (C) at serial dilutions of 1–100 μM flowed over immobilized XTX100. Assay was performed at 37°C. Calculated k_a , k_d , and K_D are reported.

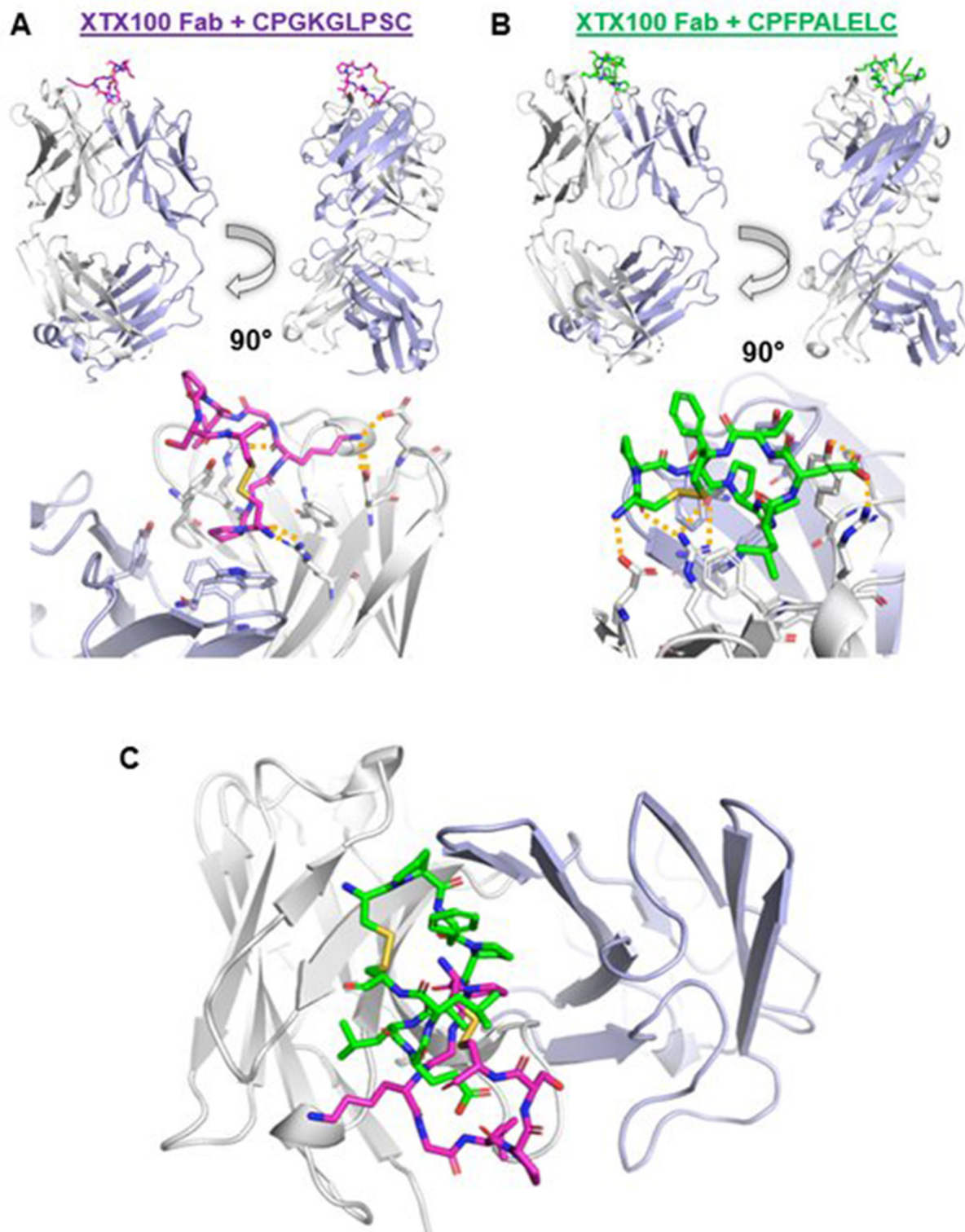


Figure 2 Crystallographic data of peptide:Fab complexes. (A) Crystal structure of XTX100_{Fab} in complex with CPGKGLPSC. Fab light and heavy chains are shown in blue and white, respectively, and peptide is shown in magenta. Key interactions shown with yellow dash lines. (B) Crystal structure of XTX100_{Fab} in complex with CPFPALELC. Fab light and heavy chains are shown in blue and white, respectively, and peptide is shown in green. (C) Mutual superposition of CPGKGLPSC (magenta) and CPFPALELC (green) in complex with XTX100_{Fab}.

SEB, in which IL-2 production is a measurement of T cell activation.³⁷ SEB-stimulated PBMC cultures treated with 40 µg/mL XTX100 and activated XTX101 demonstrated

a 11.7-fold and 12.0-fold increase in IL-2 production, respectively, over isotype mAb. Consistent with the reduced binding observed with intact XTX101, PBMCs

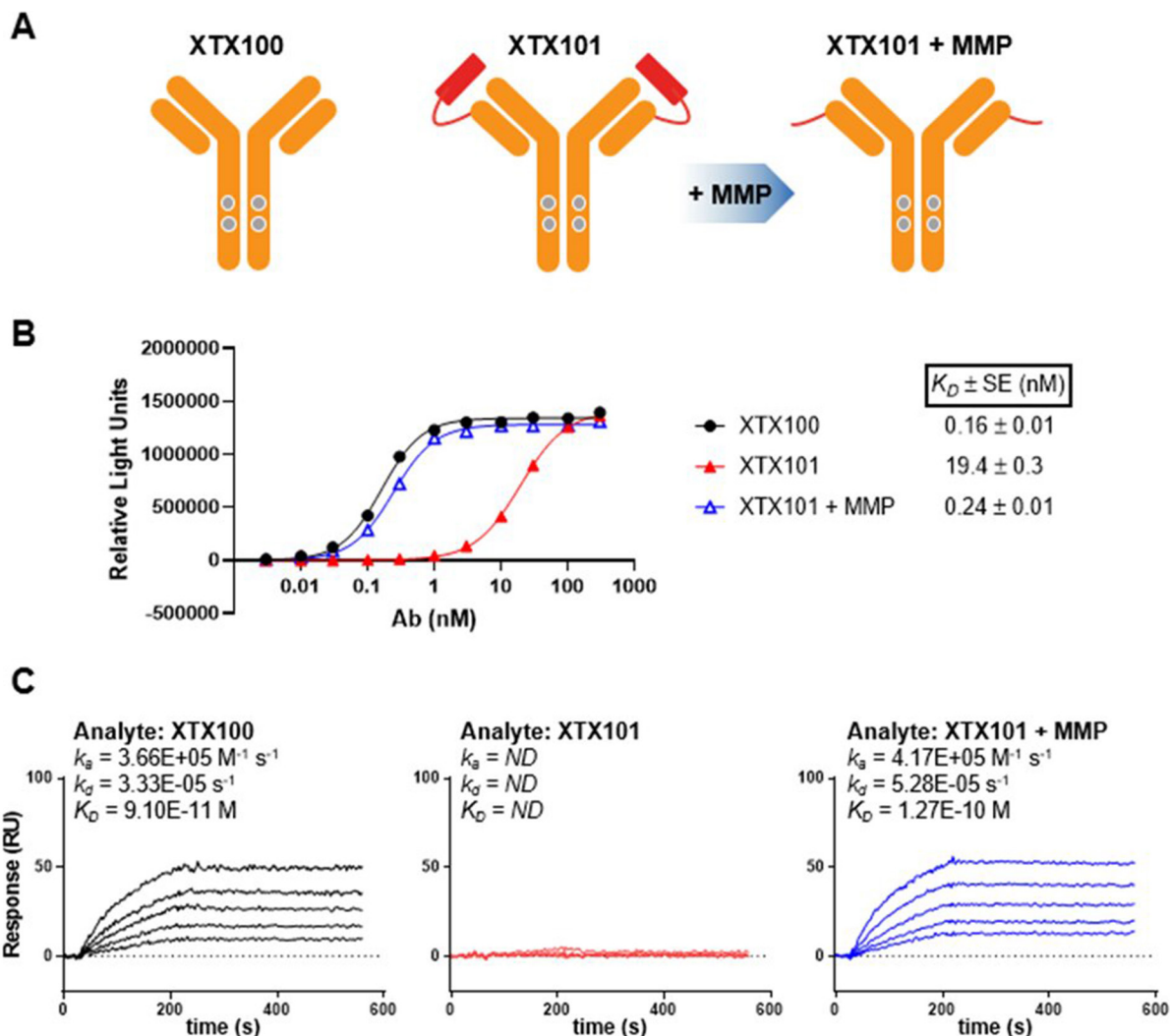


Figure 3 Design and activity of XTX101. (A) Diagram of XTX101, which consists of anti-CTLA-4 mAb XTX100 (left) covalently attached to masking peptide through a protease-sensitive linker (middle). After enzymatic activation by recombinant human MMP-9, masking peptides dissociate from the mAb, resulting in activated XTX101 (right). In vitro binding to human CTLA-4 as determined by CTLA-4 binding ELISA (B) and SPR (C), comparing intact (red) and activated XTX101 (XTX101+MMP, blue) to XTX100 (black). Calculated k_a , k_d , and K_D are reported. mAb, monoclonal antibody; ND, not determined; SPR, surface plasmon resonance.

treated with intact XTX101 exhibited a minimal (2.5-fold) increase over isotype mAb. Taken together, these studies demonstrate that intact XTX101 has reduced function in vitro relative to proteolytically activated XTX101. These data also show that proteolytic activation of XTX101 results in potency comparable to that of the unmasked parental control XTX100.

XTX101 monotherapy inhibits tumor growth and enhances survival more effectively than ipilimumab-analog in MB49 tumor model

To assess in vivo activity and tolerability of XTX101, human CTLA-4 transgenic mice were implanted with MB49 tumor cells and randomized into treatment groups when the tumors were $\sim 150 \text{ mm}^3$. Ipilimumab-analog was included as an active comparator in evaluating the TGI and survival of XTX101. XTX101 treatment resulted in significant TGI compared with isotype control, similar

TGI to unmasked XTX100, and greater survival than ipilimumab-analog (figure 5A,B). A single intravenous dose of XTX101 significantly inhibited tumor growth compared with the isotype control antibody across all tested dose levels, achieving 80.5 to 94% TGI at day 16 ($p < 0.0001$). Treatment with ipilimumab-analog (65.2% to 89.8% TGI) and XTX100 (90.4% to 94% TGI) also resulted in growth inhibition of MB49 tumors in all tested dose levels at day 16 (online supplemental table 4 and online supplemental figure 5). Statistical analysis revealed that the differences observed with all treatment groups were significant ($p = 0.0002$ ipilimumab-analog at the 1 mg/kg dose level, and $p < 0.0001$ for all other treatment groups) compared with the isotype group. At the 1 mg/kg dose level, XTX100 (94% TGI), XTX101 (80.5% TGI), and ipilimumab-analog (65.2% TGI) resulted in increased TGI relative to isotype control. At the 3 mg/

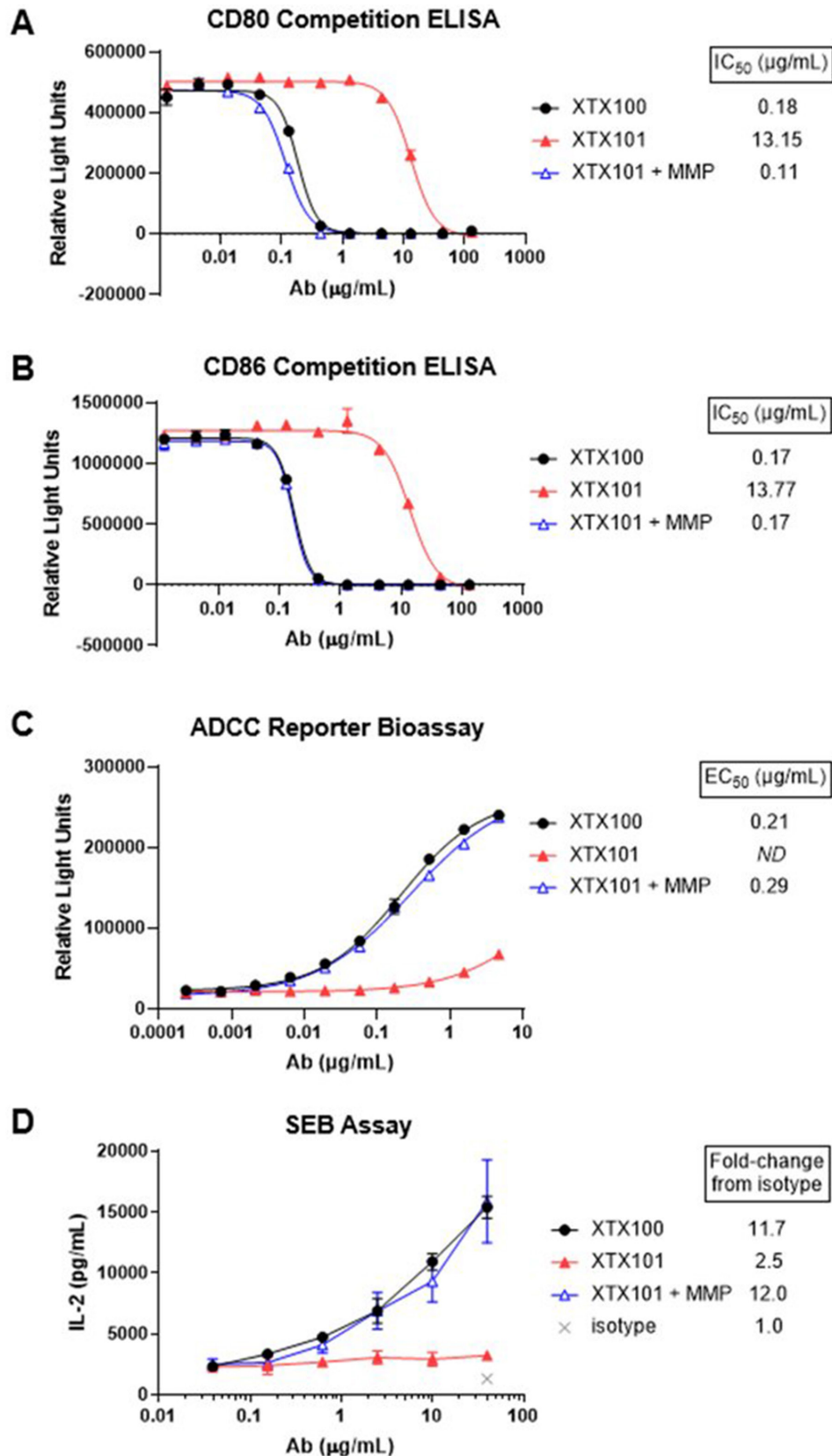


Figure 4 In vitro function of XTX101. (A,B) In vitro inhibition of human CTLA-4 binding to CD80 (A) and CD86 (B) by XTX100 (black), XTX101 (red), and activated XTX101 (blue), as assessed by ELISA. (C) In vitro activity of intact (red) and activated XTX101 (blue) compared with XTX100 (black) in antibody-dependent cellular cytotoxicity (ADCC) reporter bioassay. (D) IL-2 production of SEB-stimulated human peripheral blood mononuclear cells (PBMCs) incubated with XTX100 (black), XTX101 (red), and activated XTX101 (blue), as measured by ELISA. Fold-change from isotype at highest mAb concentration is reported. ND, not determined.

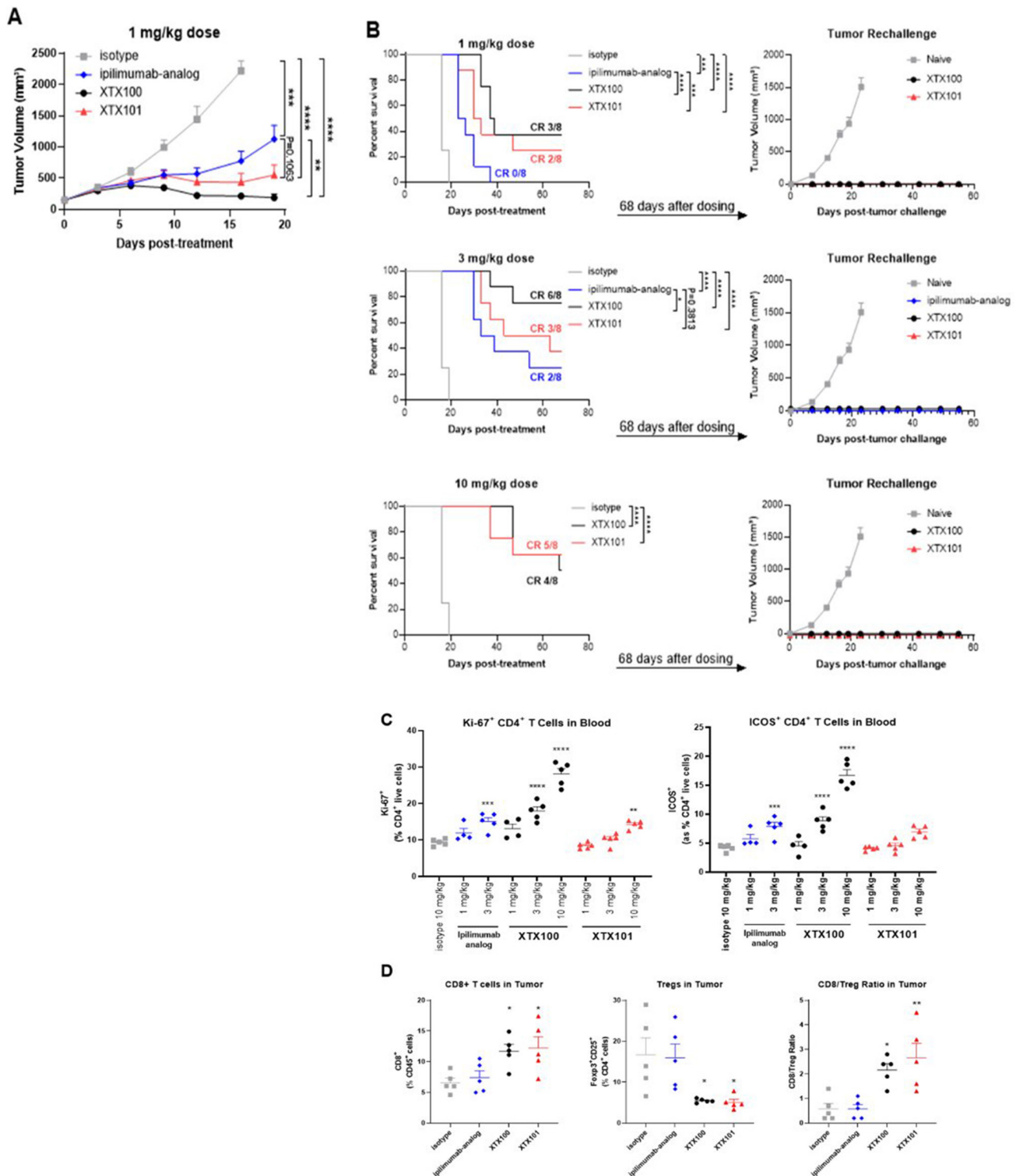


Figure 5 TTX101 monotherapy in MB49 tumor model. (A–C) For the TGI study, B-hCTLA-4 mice bearing syngeneic MB49 murine bladder carcinoma tumors (~150 mm³) were treated intravenously with a single dose of XTX100 (black), XTX101 (red), ipilimumab-analog (blue), or isotype (gray) mAb at indicated dose levels (n=8 per group). (A) Tumor volume was measured twice weekly and plotted as mean±SEM TGI from 1 mg/kg dose groups shown. Online supplemental figure 5 shows TGI from 3 and 10 mg/kg dose groups. (B) Survival curves with number of CR indicated from initial study (left), and tumor volume curves plotted as mean±SEM from tumor rechallenge study (right) for indicated dose cohorts. (C) Immunophenotypic analyses of CD45⁺ CD3⁺ CD4⁺ T cells in the peripheral blood, 5 days post-dose. (D, E) For the tumor pharmacodynamics study, B-hCTLA-4 mice bearing syngeneic MB49 murine bladder carcinoma tumors (~350 mm³) were treated intravenously with a single dose of XTX100 (black), XTX101 (red), ipilimumab-analog (blue), or isotype (gray) mAb at 3 mg/kg (n=5 per group). Immunophenotypic analyses by flow cytometry of live CD45⁺ CD3⁺ CD4⁺ Foxp3⁺ Tregs and live CD45⁺ CD3⁺ CD8⁺ T cells from spleens (D) and tumors (E) were measured on day 7. *p<0.05; **p<0.01; ***p<0.001; ****p<0.0001, compared with isotype control. TGI, tumor growth inhibition; Tregs, regulatory T cells.

kg dose level, ipilimumab-analog, XTX100, and XTX101 similarly inhibited tumor growth (89.8% to 93.9% TGI). For each dose tested, there were no significant differences between XTX100 and XTX101, indicating that XTX101 treatment resulted in similar TGI as unmasked XTX100.

Single intravenous doses of XTX101 resulted in dose-dependent complete responses in the MB49 tumor model: two out of eight mice in the 1 mg/kg group, three out of eight mice in the 3 mg/kg group and five out of eight mice in the 10 mg/kg group (figure 5B and online supplemental table 4). Similarly, the unmasked XTX100 also induced complete responses across all tested dose levels: three out of eight mice in the 1 mg/kg group, six out of eight mice in the 3 mg/kg group and four out of eight mice in the 10 mg/kg group. In contrast, ipilimumab-analog did not induce a complete response in the 1 mg/kg group and only achieved complete responses in two out of eight mice in the 3 mg/kg group. Body weight loss was not observed for any group throughout the study.

Mice with no evidence of tumors at 68 days post-treatment were subsequently rechallenged with a SC injection of MB49 tumor cells in the opposite flank. Naïve mice were also inoculated with MB49 tumor cells in the same manner as a control. Tumors grew rapidly in all naïve mice (figure 5B). In contrast, 55 days after rechallenge all treated mice (including XTX100 and ipilimumab complete responders) remained tumor-free, indicating that a single XTX101 intravenous bolus treatment generated a robust, protective antitumor immune memory.

XTX101 monotherapy demonstrates reduced T cell proliferation and activation in the blood and superior intratumoral Treg depletion compared with ipilimumab-analog in MB49 tumor model

Systemic pharmacodynamic effects of XTX100, XTX101, and ipilimumab-analog treated mice in the TGI study were evaluated on day 5 by flow cytometry-based immunophenotyping of peripheral blood. T cell proliferation and activation were assessed by measuring Ki67 and ICOS expression, respectively. XTX100 treatment resulted in significant dose-dependent increases of CD4⁺ Ki67⁺ and CD4⁺ ICOS⁺ T cells in peripheral blood at 3 mg/kg (1.9-fold and 2.1-fold, respectively) and 10 mg/kg (3-fold and 4-fold) dose levels compared with the isotype control group (figure 5C). The 3 mg/kg dose of ipilimumab-analog also significantly increased CD4⁺ Ki67⁺ (1.6-fold) and CD4⁺ ICOS⁺ (1.9-fold) T cells compared with isotype control. In contrast, 1 and 3 mg/kg of XTX101 did not significantly increase CD4⁺ Ki67⁺ T cell levels in the blood. In the 10 mg/kg groups, the increase in CD4⁺ Ki67⁺ T cells of XTX101 treated mice was significantly lower than that of XTX100 (1.5-fold vs 3-fold; $p < 0.0001$). XTX101 had no significant effect on CD4⁺ ICOS⁺ T cells at any of the doses evaluated. In summary, these data indicate that XTX101 induces minimal peripheral immune cell activation compared with unmasked XTX100 and ipilimumab-analog at corresponding dose levels.

The pharmacodynamic effect of XTX101 was further interrogated in a dedicated study utilizing human CTLA-4 transgenic mice implanted with MB49 tumor cells. Once tumors reached a mean volume of $\sim 350 \text{ mm}^3$, mice were given a single, 3 mg/kg intravenous bolus dose of XTX101, XTX100, or ipilimumab-analog ($n=5$ per group). An isotype control antibody was also dosed at 10 mg/kg. Pharmacodynamic effects of test articles were evaluated in spleens (periphery) and tumors (intratumoral) harvested on study day 7. XTX101 significantly depleted intratumoral Tregs and increased intratumoral cytotoxic CD8⁺ T cells, resulting in a fivefold increase in the CD8/Treg ratio in tumors compared with isotype (figure 5D). These observed tumor pharmacodynamic effects were similar in mice receiving XTX101 and unmasked XTX100. In contrast, ipilimumab-analog did not significantly increase intratumoral CD8⁺ T cells nor decrease Tregs. None of the treatments affected splenic Tregs nor CD8⁺ T cell numbers (online supplemental figure 6). The pharmacodynamic analyses of XTX101 revealed the tumor-specific depletion of Tregs and an increase in intratumoral CD8⁺ T cells while maintaining lower levels of non-tumor CD4⁺ T cell proliferation and activation compared with ipilimumab-analog in the MB49 model.

XTX101 and anti-PD-1 combination treatment elicits significant TGI in MC38-bearing mice

Clinically, ipilimumab plus anti-PD-1 treatment demonstrated higher efficacy than ipilimumab monotherapy in patients who are resistant to anti-PD-(L)1 treatment.³⁸ To evaluate the effect of XTX101 plus anti-PD-1 combination treatment in a preclinical PD-1 resistant mouse model, TGI was evaluated in human CTLA-4 expressing mice-bearing syngeneic MC38 murine colon carcinoma tumors. Once tumors reached $\sim 150 \text{ mm}^3$, mice were randomized into treatment groups and administered 10 mg/kg isotype control mAb, 0.3 mg/kg XTX101, 10 mg/kg anti-murine PD-1 mAb (RMP1-14), or 0.3 mg/kg XTX101 with 10 mg/kg anti-murine PD-1 mAb ($n=8$). On day 14 of the study, neither XTX101 nor anti-PD-1 mAb monotherapies exhibited significant TGI compared with isotype control group (figure 6A and online supplemental table 5). Anti-PD-1 mAb+XTX101 combination treatment resulted in a significant TGI of 82.3% on day 14 ($p=0.0002$). No body weight differences were observed between the groups throughout the study, indicating all the treatments were well tolerated (figure 6B). In total, the combination of XTX101 plus anti-PD-1 mAb showed robust TGI superior to either drug as a monotherapy with minimal systemic toxicity.

Novel ex vivo assay demonstrates the activation of XTX101 by human tumor samples

We evaluated the ability of human tumors to activate XTX101 in an ex vivo assay system (figure 7). In this system, fresh patient tumor biopsies were mechanically disaggregated and incubated in media for 1–4 days. TCM

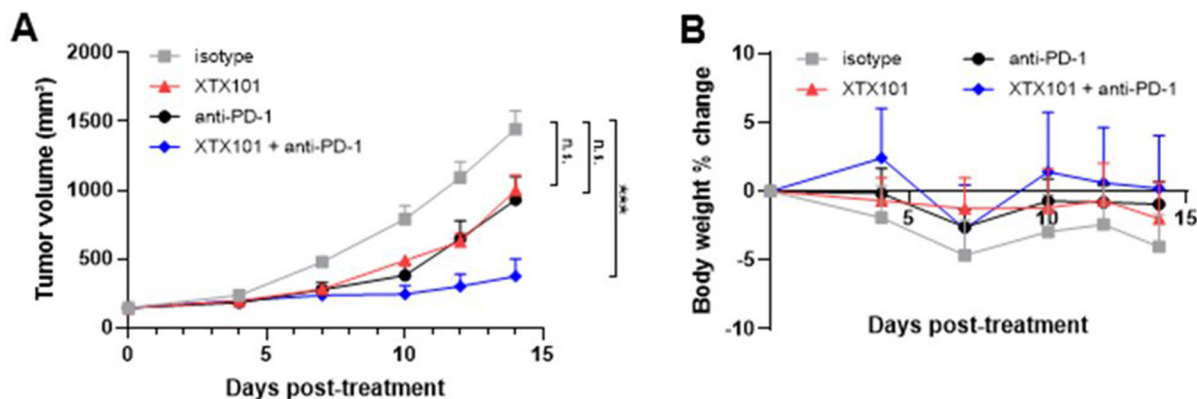


Figure 6 XTX101+anti-PD-1 combination therapy in MC38 tumor model. In vivo study was performed to evaluate the therapeutic TGI of XTX101 in combination with an anti-muPD-1 antibody RMP1-14 in B-hCTLA-4 mice bearing syngeneic MC38 murine colon carcinoma tumors (n=8 per group). Isotype control mAb and XTX101 were given to animals as a single intravenous injection on day 0, whereas anti-murine PD-1 mAb was given every 3 days (Q3D) three times by intraperitoneal injection starting on day 0. (A) Tumor volume was measured twice weekly and plotted as mean±SEM. (B) Body weight % change plotted as mean±SEM from day 0 body weight. A two-way analysis of variance with Dunnett's multiple comparisons post-test was performed (*p<0.05; **p<0.01; ***p<0.001; n.s.=not significant). mAb, monoclonal antibody; TGI, tumor growth inhibition.

was separated from cells by centrifugation, and harvested TCM was subsequently incubated with XTX101 at 37°C for 2–4 days. After incubation, the samples were tested for activation in a CTLA-4 binding ELISA. As shown in figure 7, XTX101 was activated by the majority of samples from patients with melanoma, RCC, NSCLC, ovarian, bladder, colon, breast, and liver cancers. Overall, XTX101 was activated in the ex vivo assay by 55 of 82 (67%) human tumor samples. These ex vivo experiments using TCM from eight different primary human tumor types demonstrate that XTX101 can be unmasked and proteolytically activated by proteases secreted from a broad range of solid tumor types.

DISCUSSION

Ipilimumab was the first immune checkpoint therapy for cancer treatment when it was FDA-approved for patients

with metastatic melanoma in 2011. However, toxicities arising from systemic effects of mAb therapies have limited the clinical potential of anti-CTLA-4 antibodies. Several approaches have attempted to circumvent this problem through various engineering designs. In one approach, ADG116 was designed to target a unique epitope of CTLA-4 that provides a weaker checkpoint inhibition in terms of CD80/CD86 ligand binding inhibition by CTLA-4.³⁹ In contrast, others have attempted to increase the potency of anti-CTLA-4 mAb through enhancement of Treg depletion.¹⁴ For instance, BMS-986218 and botensilimab are two anti-CTLA-4 mAbs with Fc regions engineered to increase binding affinity to Fcγ receptors, thereby enhancing ADCC.^{20–21} Phase I clinical trials with monotherapy ADG116, BMS-986218, or botensilimab, however, have resulted in severe adverse events for many patients.^{40–42} These clinical results indicate

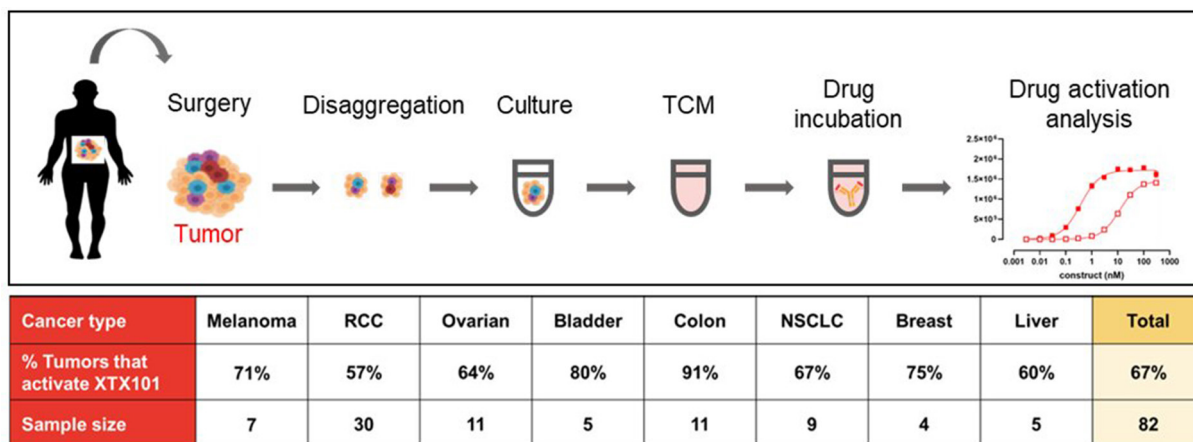


Figure 7 XTX101 was activated by human tumor samples in an ex vivo assay. Resected biopsy tumor samples from human patients of listed indications were mechanically disaggregated and cultured in medium for 1–4 days. The supernatant was harvested and incubated with XTX101 for 2–4 days. After incubation, XTX101 was assessed for activation, as determined by CTLA-4 binding ELISA. NSCLC, non-small cell lung cancer; RCC, renal cell carcinoma; TCM, tumor conditioned media.

increasing the potency through enhanced ADCC potential of a constitutively active anti-CTLA-4 mAb result in a shift, not an expansion, of the therapeutic index. We, as well as others, are attempting to expand the therapeutic index by focusing the activity of an anti-CTLA-4 mAb solely within the TME.^{30 43 44}

We have generated and characterized XTX101, a tumor-activated, Fc enhanced anti-CTLA-4 mAb that leverages the local dysregulation and increased activity of proteases within the TME to activate the Fc-enhanced CTLA-4 antagonist. In mice, this results in intratumoral Treg depletion, TGI, and reduction of the on-target/off-tumor activity observed with constitutively active checkpoint inhibitor mAbs XTX100 and ipilimumab-analog. XTX101 was designed using a structurally informed approach, as crystallographic data aided in the design of the protease-sensitive linker connecting the peptide mask to the mAb. Successful masking was confirmed in initial SPR studies, in which intact XTX101 demonstrated negligible binding to human CTLA-4. In the same assay, XTX101 preactivated by recombinant MMP displayed affinity for CTLA-4 comparable to that of unmasked parental XTX100. The activation-dependent function of XTX101 was also confirmed in *in vitro* studies, including CD80/CD86 competition assays, reporter cell assays, and an activation assay of human PBMCs. In a mouse syngeneic MB49 tumor model, XTX101 monotherapy demonstrated superior survival to that of ipilimumab-analog. A single dose of 1 mg/kg XTX101 exhibited equivalent TGI to that of 3 mg/kg ipilimumab-analog, suggesting that XTX101 has enhanced potency compared with ipilimumab-analog. Flow cytometry data demonstrated equivalent levels of Ki-67⁺ CD4⁺ T cells in the blood of mice dosed with 3 mg/kg ipilimumab-analog and 10 mg/kg XTX101, indicating that XTX101 has lower systemic pharmacodynamic effect than ipilimumab-analog. Taken together, these two preclinical datasets suggest that XTX101 may possess a significantly wider therapeutic index compared with ipilimumab-analog.

In preclinical studies performed by other groups, Treg depletion by anti-CTLA-4 therapy was sufficient for potent TGI (reviewed in previous work⁴⁵). Mutations were incorporated within the Fc region of our anti-CTLA-4 mAb to increase affinity for human FcγRIIIa/murine FcγRIII³² and enhance depletion of Tregs, which resulted in superior intratumor Treg depletion by XTX100 and XTX101 over ipilimumab-analog in our MB49 mouse study. The observed increase in peripheral CD4⁺ T cell proliferation and activation in mice treated with unmasked XTX100 highlights the advantage for a masked, tumor-activated anti-CTLA-4 mAb. In contrast to the observed increase in CD4⁺ T cell proliferation in the blood after administration of unmasked XTX100, changes in peripheral CD4⁺ T cells were significantly reduced in mice treated with equivalent dose levels of XTX101, demonstrating successful masking of XTX101 *in vivo*.

Ipilimumab in combination with the anti-PD-1 antibody nivolumab has received FDA approval for multiple

indications including melanoma and NSCLC. A recent meta-analysis of the risk of irAEs among patients with advanced cancers receiving ipilimumab+nivolumab combination therapy concluded that the combination therapy increased the incidence of irAEs.⁴⁶ We assessed the TGI of XTX101 in combination with anti-PD-1 treatment in the MC38 mouse tumor model. Significant anti-tumor effects were observed with the XTX101+anti-PD-1 mAb combination therapy, whereas the monotherapies provided suboptimal TGI. No body weight loss occurred in any treatment group, thereby indicating that the combination of XTX101 and anti-PD-1 mAb did not manifest overt toxicities in mice.

In the MB49 murine tumor model, the minimal activation of peripheral T cells demonstrated XTX101 remained masked in circulation, whereas the increased intratumoral CD8:Treg ratio indicated activation of XTX101 within the TME. One limitation of these murine tumor models is the difficulty to translate data to human patients as relative concentrations of proteases could be different between species. To address this question, studies were performed to test activation of XTX101 by human tumor samples *ex vivo*. We observed activation of XTX101 in TCM collected from the majority (67%) of fresh tumor biopsy samples. Importantly, the tumor samples spanned eight distinct tumor types, suggesting that XTX101 could have activity across multiple cancer indications. Of note, the *ex vivo* assay utilizes a cell-free system and thus does not capture activation by membrane-bound proteases commonly present in the TME. Despite the exclusion of membrane-bound proteases, activation of XTX101 was still observed across all tested indications. The activation by human tumor samples in the *ex vivo* assay system may therefore underestimate the potential for activation of XTX101 by human tumors in patients.

Taken together, these preclinical data suggest that XTX101 is selectively active in the TME as intended. Currently, XTX101 is being evaluated in an ongoing phase 1/2 trial (ClinicalTrials.gov Identifier: NCT04896697) with the initial safe starting dose determined by using industry standard practice and based on the highest non-severely toxic dose from a GLP repeat dose toxicology study in cynomolgus monkeys.

Acknowledgements We thank Simon Tomlinson for initial resource and funding acquisition, Tim Miles and Asaul Gonzalez for methodology development, Conn Mallett and Zoe Navapanich for crystallization and data collection, and C. Uli Bialucha for editorial support.

Contributors KAJ: Conceptualization, data curation, formal analysis, investigation, methodology, project administration, supervision, visualization, writing-original draft, writing-review/editing, and guarantor. MP: Conceptualization, data curation, investigation, methodology, resources, supervision, visualization, and writing-review/editing. MP-R: Data curation, formal analysis, investigation, methodology, supervision, visualization, writing-review/editing. UE: Data curation, formal analysis, investigation, methodology, supervision, visualization, and writing-review/editing. PJ: Data curation, formal analysis, investigation, methodology, and visualization. WG: Data curation, formal analysis, investigation, methodology, and visualization. MM: Data curation, investigation, methodology, and visualization. DM-L: Data curation, investigation, resources, and supervision. CO'T: Data curation and investigation. ZL: Data curation and investigation. BN: supervision and writing-review/editing. VF: Investigation and resources. HQ: Resources, supervision, and

writing-review/editing. TC: Project administration, supervision, and writing-review/editing. RCO'H: Project administration, supervision, writing-review/editing. UR: Conceptualization, funding acquisition, methodology, and supervision. MK: Data curation, investigation, methodology, project administration, resources, supervision, and writing-review/editing. JO'N: Data curation, project administration, supervision, visualization, and writing-review/editing. JCW: Conceptualization, data curation, funding acquisition, methodology, project administration, supervision, visualization, and review and editing.

Funding Research and analysis were supported by Xilio Therapeutics, Inc. Research reported in this publication included work performed at the City of Hope Drug Discovery and Structural Biology shared resource facility, supported by the National Institutes of Health under award number P30CA033572.

Disclaimer The content is solely the responsibility of the authors and does not represent the official views of the National Cancer Institute or the National Institutes of Health. The authors were responsible for all content and received no honoraria for development of this article.

Competing interests KAJ, MP-R, UE, PJ, WG, MM, DM-L, CO'T, ZL, BN, HQ, TC, RCO'H, MK, and JO'N report personal fees from Xilio Therapeutics during the conduct of the study. UR and JCW are co-founders, shareholders, and consultants to Xilio Therapeutics.

Patient consent for publication Not applicable.

Ethics approval Not applicable.

Provenance and peer review Not commissioned; externally peer reviewed.

Data availability statement All data relevant to the study are included in the article or uploaded as supplemental information.

Supplemental material This content has been supplied by the author(s). It has not been vetted by BMJ Publishing Group Limited (BMJ) and may not have been peer-reviewed. Any opinions or recommendations discussed are solely those of the author(s) and are not endorsed by BMJ. BMJ disclaims all liability and responsibility arising from any reliance placed on the content. Where the content includes any translated material, BMJ does not warrant the accuracy and reliability of the translations (including but not limited to local regulations, clinical guidelines, terminology, drug names and drug dosages), and is not responsible for any error and/or omissions arising from translation and adaptation or otherwise.

Open access This is an open access article distributed in accordance with the Creative Commons Attribution Non Commercial (CC BY-NC 4.0) license, which permits others to distribute, remix, adapt, build upon this work non-commercially, and license their derivative works on different terms, provided the original work is properly cited, appropriate credit is given, any changes made indicated, and the use is non-commercial. See <http://creativecommons.org/licenses/by-nc/4.0/>.

ORCID iDs

Kurt A Jenkins <http://orcid.org/0000-0003-2834-7068>

John C Williams <http://orcid.org/0000-0002-0522-384X>

REFERENCES

- 1 Wolchok JD, Hodi FS, Weber JS, *et al.* Development of Ipilimumab: a novel Immunotherapeutic approach for the treatment of advanced melanoma. *Ann N Y Acad Sci* 2013;1291:1–13.
- 2 Harper K, Balzano C, Rouvier E, *et al.* CTLA-4 and CD28 activated lymphocyte molecules are closely related in both mouse and human as to sequence, message expression, gene structure, and chromosomal location. *J Immunol* 1991;147:1037–44.
- 3 Dariavach P, Mattéi MG, Golstein P, *et al.* Human IG Superfamily CTLA-4 gene: chromosomal localization and identity of protein sequence between murine and human CTLA-4 cytoplasmic domains. *Eur J Immunol* 1988;18:1901–5.
- 4 Collins AV, Brodie DW, Gilbert RJC, *et al.* The interaction properties of costimulatory molecules revisited. *Immunity* 2002;17:201–10.
- 5 Krummel MF, Allison JP. CD28 and CTLA-4 have opposing effects on the response of T cells to stimulation. *J Exp Med* 1995;182:459–65.
- 6 Walunas TL, Lenschow DJ, Bakker CY, *et al.* CTLA-4 can function as a negative regulator of T cell activation. *Immunity* 1994;1:405–13.
- 7 Grosso JF, Jure-Kunkel MN. CTLA-4 blockade in tumor models: an overview of preclinical and translational research. *Cancer Immunol* 2013;13:5.
- 8 Hamid O, Schmidt H, Nissan A, *et al.* A prospective phase II trial exploring the association between tumor microenvironment biomarkers and clinical activity of Ipilimumab in advanced melanoma. *J Transl Med* 2011;9:204.
- 9 Lebbé C, Meyer N, Mortier L, *et al.* Evaluation of two dosing regimens for Nivolumab in combination with Ipilimumab in patients with advanced melanoma: results from the phase IIIB/IV checkmate 511 trial. *J Clin Oncol* 2019;37:867–75.
- 10 Wolchok JD, Neyns B, Linette G, *et al.* Ipilimumab monotherapy in patients with pretreated advanced melanoma: a randomised, double-blind, multicentre, phase 2, dose-ranging study. *Lancet Oncol* 2010;11:155–64.
- 11 Xu H, Tan P, Zheng X, *et al.* Immune-related adverse events following administration of anti-cytotoxic T-lymphocyte-associated Protein-4 drugs: a comprehensive systematic review and meta-analysis. *Drug Des Devel Ther* 2019;13:2215–34.
- 12 Ascierto PA, Del Vecchio M, Robert C, *et al.* Ipilimumab 10 mg/kg versus Ipilimumab 3 mg/kg in patients with unresectable or metastatic melanoma: a randomised, double-blind, Multicentre, phase 3 trial. *Lancet Oncol* 2017;18:611–22.
- 13 Simpson TR, Li F, Montalvo-Ortiz W, *et al.* Fc-dependent depletion of tumor-infiltrating regulatory T cells co-defines the efficacy of anti-CTLA-4 therapy against Melanoma. *J Exp Med* 2013;210:1695–710.
- 14 Sharma A, Subudhi SK, Blando J, *et al.* Anti-CTLA-4 immunotherapy does not deplete Foxp3(+) regulatory T cells (Tregs) in human cancers. *Clin Cancer Res* 2019;25:3469–70.
- 15 Arce Vargas F, Furness AJS, Litchfield K, *et al.* Fc Effector function contributes to the activity of human anti-CTLA-4 antibodies. *Cancer Cell* 2018;33:649–63.
- 16 Selby MJ, Engelhardt JJ, Quigley M, *et al.* Anti-CTLA-4 antibodies of IgG2A isotype enhance antitumor activity through reduction of Intratumoral regulatory T cells. *Cancer Immunol Res* 2013;1:32–42.
- 17 Bulliard Y, Jolicoeur R, Windman M, *et al.* Activating FC gamma receptors contribute to the antitumor activities of Immunoregulatory receptor-targeting antibodies. *J Exp Med* 2013;210:1685–93.
- 18 Quezada SA, Peggs KS. Lost in translation: deciphering the mechanism of action of anti-human CTLA-4. *Clin Cancer Res* 2019;25:1130–2.
- 19 El-Khoueiry AB, Fakih MG, Gordon MS, *et al.* Results from a phase 1A/1B study of Botensilimab(BOT), a novel innate/adaptive immune activator, plus Balstilimab (BAL; anti-PD-1 antibody) metastatic heavily pretreated Microsatellite stable colorectal cancer (MSS CRC) [Powerpoint presentation]. ASCO Gastrointestinal Cancers Symposium; San Francisco, CA, 2023
- 20 Engelhardt J, Akter R, Loffredo J, *et al.* K., editor abstract 4552: preclinical characterization of BMS-986218, a novel Nonfucosylated anti-CTLA-4 antibody designed to enhance antitumor activity. *Cancer Research* 2020;80:4552.
- 21 Waight JD, Chand D, Dietrich S, *et al.* Selective Fcγ3R Co-engagement on APCs modulates the activity of therapeutic antibodies targeting T cell antigens. *Cancer Cell* 2018;33:1033–47.
- 22 Sevenich L, Joyce JA. Pericellular proteolysis in cancer. *Genes Dev* 2014;28:2331–47.
- 23 Egeblad M, Werb Z. New functions for the matrix metalloproteinases in cancer progression. *Nat Rev Cancer* 2002;2:161–74.
- 24 Kessenbrock K, Plaks V, Werb Z. Matrix metalloproteinases: regulators of the tumor microenvironment. *Cell* 2010;141:52–67.
- 25 Dudani JS, Warren AD, Bhatia SN. Harnessing protease activity to improve cancer care. *Annu Rev Cancer Biol* 2018;2:353–76.
- 26 Turk BE, Huang LL, Piro ET, *et al.* Determination of protease cleavage site motifs using mixture-based oriented peptide libraries. *Nat Biotechnol* 2001;19:661–7.
- 27 Cieplak P, Strongin AY. Matrix metalloproteinases - from the cleavage data to the prediction tools and beyond. *Biochim Biophys Acta Mol Cell Res* 2017;1864:1952–63.
- 28 Isaacson KJ, Martin Jensen M, Subrahmanyam NB, *et al.* Matrix-metalloproteinases as targets for controlled delivery in cancer: an analysis of upregulation and expression. *J Control Release* 2017;259:62–75.
- 29 Prudova A, auf dem Keller U, Butler GS, *et al.* Multiplex N-Terminome analysis of MMP-2 and MMP-9 substrate Degradomes by iTRAQ-TAILS quantitative Proteomics. *Mol Cell Proteomics* 2010;9:894–911.
- 30 Kavanaugh WM. Antibody prodrgs for cancer. *Expert Opin Biol Ther* 2020;20:163–71.
- 31 Donaldson JM, Kari C, Fragoso RC, *et al.* Design and development of masked therapeutic antibodies to limit off-target effects: application to anti-EGFR antibodies. *Cancer Biol Ther* 2009;8:2147–52.
- 32 Lazar GA, Dang W, Karki S, *et al.* Engineered antibody FC variants with enhanced effector function. *Proc Natl Acad Sci U S A* 2006;103:4005–10.
- 33 Copeland RA. *Enzymes: a practical introduction to structure, mechanism, and data analysis*. 2nd ed. New York: Wiley, 2000.

- 34 Percie du Sert N, Hurst V, Ahluwalia A, *et al.* The ARRIVE guidelines 2.0: updated guidelines for reporting animal research. *BMJ Open Sci* 2020;4:e100115.
- 35 Brunet JF, Denizot F, Luciani MF, *et al.* A new member of the immunoglobulin Superfamily--CTLA-4. *Nature* 1987;328:267–70.
- 36 Bristol Myers Squibb. *Yervoy (ipilimumab)*. New York City, NY, 2021.
- 37 Selby MJ, Engelhardt JJ, Johnston RJ, *et al.* Preclinical development of Ipilimumab and Nivolumab combination Immunotherapy: Mouse tumor models. In vitro functional studies, and cynomolgus macaque toxicology. *PLoS One* 2016;11:e0167251.
- 38 Pires da Silva I, Ahmed T, Reijers ILM, *et al.* Ipilimumab alone or Ipilimumab plus anti-PD-1 therapy in patients with metastatic Melanoma resistant to anti-PD-(L)1 monotherapy: a multicentre, retrospective, cohort study. *Lancet Oncol* 2021;22:836–47.
- 39 Liu GD, She F, Luo K. *Development of a novel antagonist anti-CTLA-4 antibody for cancer immunotherapy*. National Harbor, MD: SITC, 2019.
- 40 Richardson GT, Parnis F, Park J, *et al.* Phase 1 dose-finding study of a novel anti-CTLA-4 antibody Adg116 as monotherapy in patients with advanced solid tumors. EMSO IO Congress; 2021
- 41 Friedman C, Ascierto P, Davar D, *et al.* 393 First-in-human phase 1/2a study of the novel nonfucosylated anti-CTLA-4 monoclonal antibody BMS-986218 ± nivolumab in advanced solid tumors: initial phase 1 results. 35th Anniversary Annual Meeting (SITC 2020); November 2020:Suppl
- 42 El-Khoueiry A, Bullock A, Tsimberidou A, *et al.* 479 AGen1181, an FC-enhanced anti-CTLA-4 antibody, alone and in combination with Balstilimab (anti-PD-1) in patients with advanced solid tumors: initial phase I results. *J Immunother Cancer* 2021;9:A509.
- 43 Engelhardt J, Akter R, Loffredo J, *et al.* Abstract 4551: preclinical characterization of novel anti-CTLA-4 prodrug antibodies with an enhanced therapeutic index. *Cancer Res* 2020;80:4551.
- 44 Pai C-C, Simons DM, Lu X, *et al.* Tumor-conditional anti-CTLA4 Uncouples antitumor efficacy from immunotherapy-related toxicity. *J Clin Invest* 2019;129:349–63.
- 45 Hong MMY, Maleki Vareki S. Addressing the elephant in the immunotherapy room: Effector T-cell priming versus depletion of regulatory T-cells by anti-CTLA-4 therapy. *Cancers (Basel)* 2022;14:1580.
- 46 Zhou S, Khanal S, Zhang H. Risk of immune-related adverse events associated with Ipilimumab-plus-Nivolumab and Nivolumab therapy in cancer patients. *Ther Clin Risk Manag* 2019;15:211–21.